Current Biology, Volume *21*

Supplemental Information

Single-Unit Responses Selective for Whole Faces in the Human Amygdala

Ueli Rutishauser, Oana Tudusciuc, Dirk Neumann, Adam N. Mamelak, A. Christopher Heller, Ian B. Ross, Linda Philpott, William Sutherling, and Ralph Adolphs

Supplemental Inventory

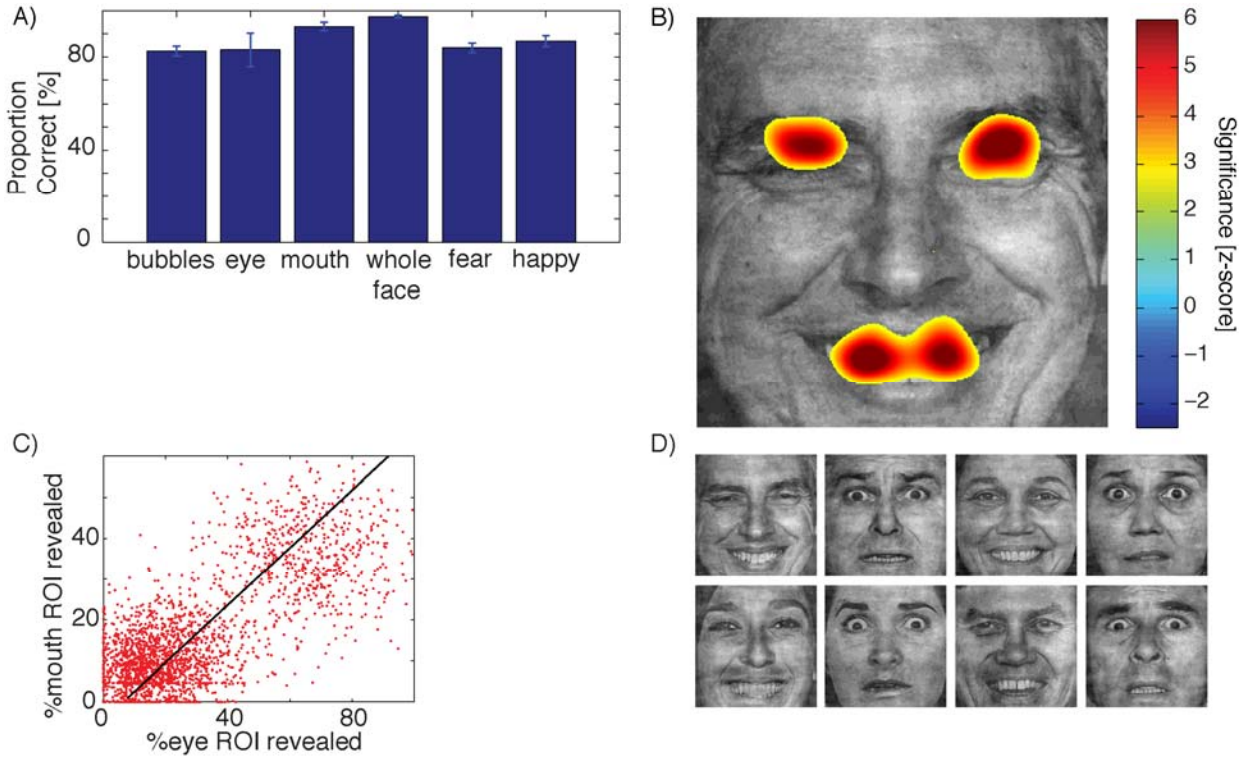

Figure S1. Further Behavioral Results and Stimulus Properties, Related to Figure 1

(A) Percentage of correct trials for the different target categories.

(B) Statistically thresholded overlay of the significant parts ($T>2.96$; $p<0.05$) of the classification image in Fig. 1C.

(C) Quantification of the bubble masks. Revealed parts of faces were distributed randomly and independently, and thus the proportion of the eye and mouth ROIs that are revealed are positively correlated (n=12950 trials, $R^2=0.60$, $p<0.001$).

(D) The face images that were used, consisting of 4 different identities (2 male, 2 female) each happy and fearful, resulting in 8 different images. Each of these was also mirror flipped, for a total of 16 images.

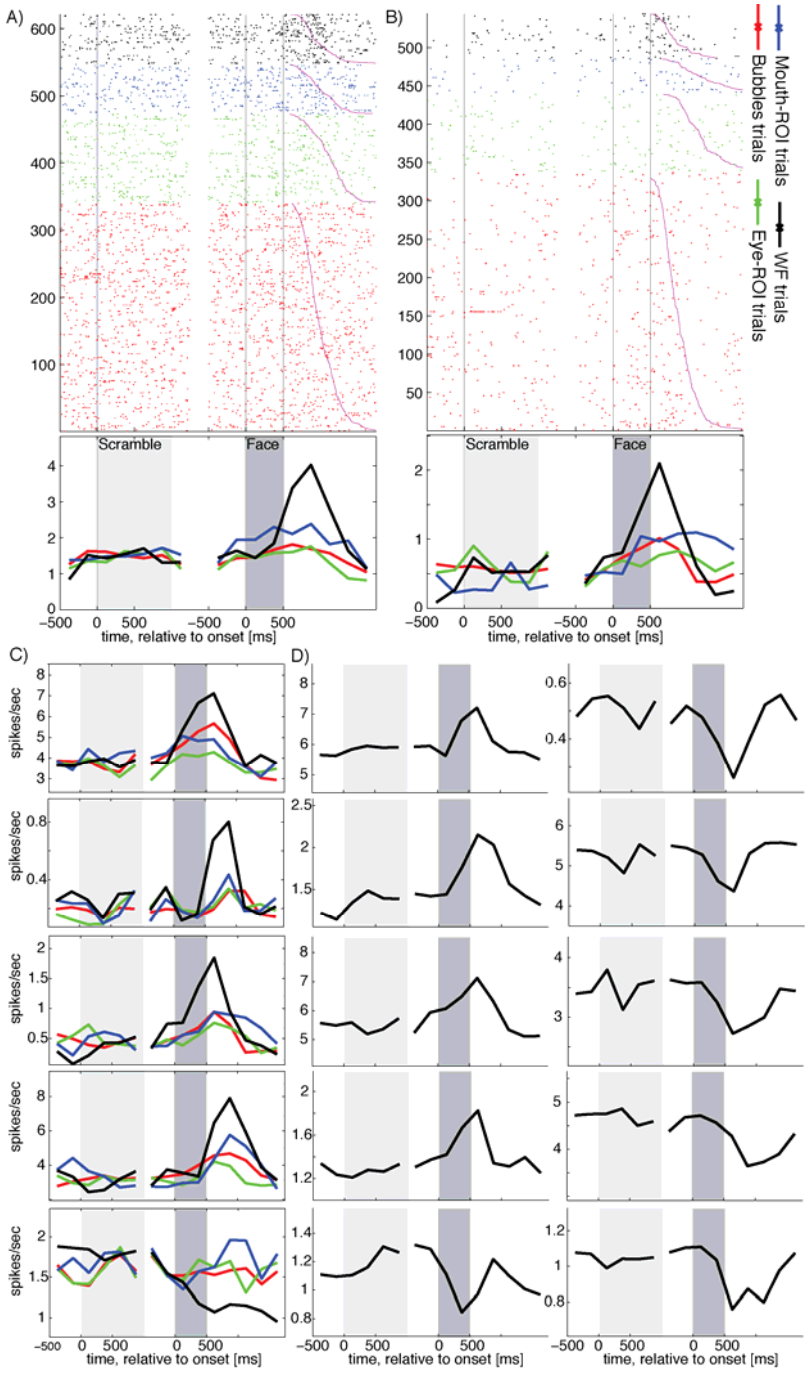

Figure S2, Related to Figure 2.

(A and B) Raster (top) and PSTH (bottom) for the units shown in Fig 2 C,D. See legend of Fig 2 for notation.

(C) Other examples of WF-selective units. See panel (B) for color-code and notation.

(D) Examples of non-WF-selective units that were responding to the face-stimulus onset (see Table S2, 2nd row). Shown is the mean response to all trial types pooled. The first 4 examples significantly increase their rate relative to the scramble vs the last 6 examples significantly decrease their rate.

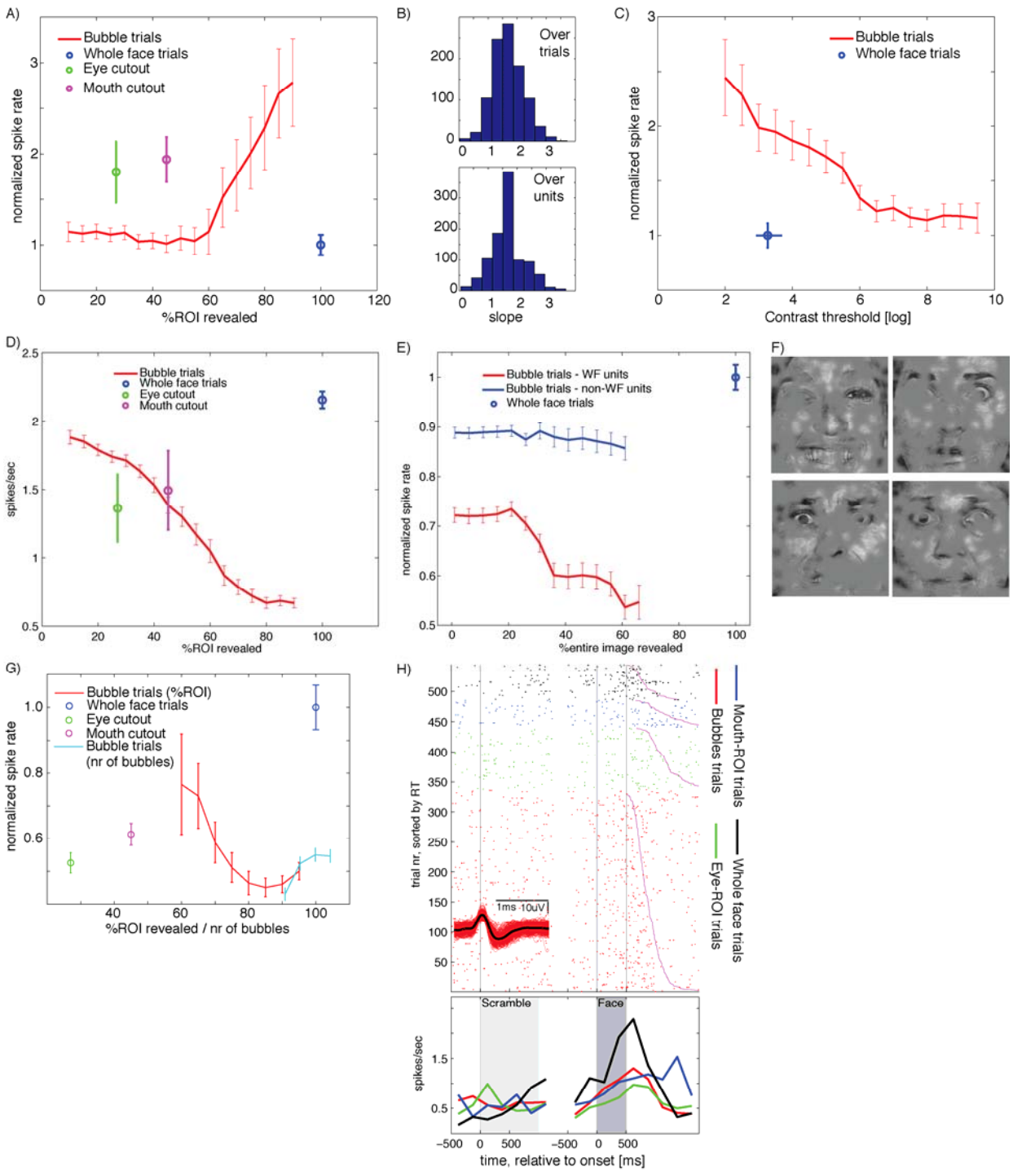
A)
Bubble trials
Whole face trials
Eye cutout
Mouth cutout
normalized spike rate
%ROI revealed
B)
Over trials
Over units
slope
C)
Bubble trials
Whole face trials
normalized spike rate
Contrast threshold [log]
D)
Bubble trials
Whole face trials
Eye cutout
Mouth cutout
spikes/sec
%ROI revealed
E)
Bubble trials - WF units
Bubble trials - non-WF units
Whole face trials
normalized spike rate
%entire image revealed
F)
G)
Bubble trials (%ROI)
Whole face trials
Eye cutout
Mouth cutout
Bubble trials
(nr of bubbles)
normalized spike rate
%ROI revealed / nr of bubbles
H)
trial nr, sorted by RT
1ms 10uV
Bubbles trials
Mouth-ROI trials
Eye-ROI trials
Whole face trials
Scramble
Face
spikes/sec
time, relative to onset [ms]

Figure S3, Related to Figure 4.

Population response of whole-face selective neurons that decrease their firing rate to whole faces (A-C), alternative measures for increasing-rate units (D-E) and response to dense bubbles (F-H).

(A and B) Population responses of all whole-face selective neurons that decrease their response to whole faces (n=4 units). The slope is significantly positive (linear regression, $p<0.001$), as verified by using a bootstrap analysis that permuted over trials or neurons (B; see Legend to main Figure 4 for analogous analysis). Note how, when the stimulus becomes more similar to a whole face, the rate increases and thus makes the response more dissimilar from a true whole face.

(C) The difference in population response in (A) could not be explained as a function of visibility (notice the location of the whole faces with respect to the bubbled trials). (D-E) Alternative measures of quantifying the relationship between revealed part of the stimulus and the neuronal response.

(D) Population responses of all whole-face selective neurons that increase their response to whole faces (n=32). Same data as shown in Fig 4C, but for absolute firing rates rather than normalized rates. The slope of the curve is -1.7 and significantly negative ($p<1e-50$) as shown as well as bootstrapped over trials and units (-1.7±0.1 and -1.7±0.6, respectively).

(E) Normalized response as a function of the proportion of the entire image that was revealed for WF (red) and non-WF (blue units). For WF units, the more of the face was revealed, the less the WF units responded (significantly negative slope, -0.3, $p<1e-29$). For non-WF units, the slope was not significantly different from zero. Compare to Fig 4C. (F-H) Response to dense bubbles in one patient (n=5 units, all increasing their firing rate for WFs).

(F) Example stimuli with approximately 100 bubbles revealed (actual stimuli from this session).

(G) Average non-linear response profile of these 5 neurons (all increased their rate for whole faces), as a function of %ROI revealed (red) and number of bubbles revealed (cyan), calculated for all trials (including the first 150, since learning was disabled). The slope of the normalized response as a function of %ROI revealed (red) was -0.45 and significantly negative ($p=0.003$). The slope of the normalized response as a function of nr bubbles (cyan) was negligible but slightly positive (0.007, $p=0.0001$). Note that the x-axis has two independent measures: %ROI for the red line and number of bubbles for the cyan curve. Also note that the two measures are not equal, i.e. 100 bubbles revealed does not correspond to 100% ROI revealed.

(H) Spiking response of an example single unit, also shown in Fig 4B4. All error bars are ±s.e.m. over trials.

Table 1. List of Patient Demographics, Pathology, and Neuropsychological Evaluation

ID	Age	Sex	Hand	Lang Dom	Benton	Epilepsy diagnosis	WAIS-III					Rey-O		
							PIQ	VIQ	VCI	POI	FSIQ	copy	IR	DR
P17	19	M	R	L	43	Left inferior frontal	128	131	122	133	134	34	23	21
P18	40	M	R	L	52	Right mesial temporal hippocampus	69	n/a	n/a	n/a	n/a	n/a	n/a	n/a
P19	34	M	R	n/a	39	Left supplementary motor neocortex	81	74	76	80	86	31	23	20.5
P20	27	M	R	L	49	Right mesial temporal hippocampus	88	98	89	101	81	33	21	23.5
P21	20	M	R	n/a	45	Right dorsolateral neocortex	n/a	n/a	93	89	n/a	34	27.5	27
P23	35	M	R	L	41	Left mesial temporal amygdala	n/a	n/a	74	86	n/a	34	n/a	9.5
P25	31	M	R	L	47	Right dorsolateral neocortex	81	91	98	82	87	36	9	5
P27	41	M	R	n/a	49	Bilateral independent temporal lobe	86	91	86	88	89	36	5	5
P28	23	M	R	L	47	Right mesial temporal hippocampus	79	77	78	80	76	34	9.5	13
P29	18	F	L	L	49	Left deep insula	104	110	107	101	107	36	19.5	19.5

Abbreviations: Hand: Dominant handedness; Lang Dom: language dominance as determined by Sodium Amybarbital (Wada) test; Benton: Benton Facial Recognition Test, long form score; WAIS-III: IQ scores from the Wechsler Adult Intelligence Scale: performance IQ (PIQ), verbal IQ (VIQ), full scale IQ (FSIQ), perceptual organization index (POI), verbal comprehension index (VCI). Benton scores 41-54 are in the normal range. Tests indicated with n/a were not performed for clinical reasons. Rey-Osterrieth Complex Figures test are raw scores, subtests are copy, immediate recall reproduction (IR), and 30-minute delayed recall reproduction (DR). 36 possible points for each, 18+ is normal depending on age. Patients 20, 21 and 27 only contributed behavior (no neurons).

Table 2. Summary of Neuronal Response Characteristics

Response Characteristics	# units	% units
Visually responsive (scramble vs. baseline blank screen)	21 total, 9 increase 12 decrease	11.4%
Face responsive (face stimulus vs. scramble, all trial categories pooled)	95 total, 34 increase 61 decrease	51.4%
Bubbled face responsive (bubble trials vs. scramble)	68	36.8%
Whole face responsive (vs. scramble)	44	23.8%
Eye cutout responsive (vs. scramble)	26	14.1%
Mouth cutout responsive (vs. scramble)	37	20.0%
Whole-face (WF) selective (vs. eye and mouth cutouts)	36	19.5%
Eye vs. mouth cutout selective	12	6.5%
Bubbles selective (vs. cutouts)	18	9.7%
Fear vs. happy (whole face trials, only for whole-face selective units)	4 / 39	10.3%
Fear vs. happy (bubbles trials, only for whole-face selective units)	8 / 39	20.5%
Identity (1-way ANOVA, 4 identities, bubbles trials)	12	6.5%
Gender X Fear/Happy (2x2 ANOVA) (gender, emotion (fear vs. happy), interaction; bubbles trials)	13, 23, 14	7.0%, 12.4%, 7.6%

All percentages are derived from a total of 185 units except when indicated otherwise. Comparisons between baseline and scramble as well as scramble and face stimuli were performed using a two-tailed paired t-test at $p<0.05$. For the pre vs. post stimulus onset comparisons for scrambles and faces (first two rows), the number of units that respond with an increase and decrease at stimulus onset, relative to pre-stimulus, are listed as well. Comparisons between different categories of face stimuli were performed using one-way ANOVAs at $p<0.05$ for the post-stimulus onset firing rates, regardless of their response relative to baseline. The shaded row indicates the condition used to identify WF-selective units (WF vs cutout trials). For comparison, the condition WF vs. bubbles (which was not used to classify the units as WF-selective) yielded 39 units. Of those, 24 are the same as in the original WF vs. cutouts condition that we used.

Supplemental Experimental Procedures

Patients

Intracranial single-unit recordings were obtained from 10 neurosurgical inpatients (Table 1) who had chronically implanted depth electrodes in the amygdalae as previously described [1, 2]. Electrodes were placed using orthogonal trajectories, and utilized to localize seizures for possible surgical treatment of epilepsy. We included only participants who had normal or corrected-to-normal vision, intact ability to discriminate faces on the Benton Facial Discrimination Task [3], and who were fully able to understand the task. Patients were tapered off any anti-seizure medication after electrode implantation over the course of several days. With some exceptions, patients were typically not on anti-convulsants anymore by the time the recordings were performed (typically 3-5 days after implantation) but might still be on other medications not related to epilepsy. All participants provided written informed consent according to protocols approved by the Institutional review boards of the Huntington Memorial Hospital and the California Institute of Technology.

Electrophysiology

We recorded bilaterally from implanted depth electrodes in the amygdala. Target locations were verified using post-implantation structural MRIs as shown in [1]. At each site, we recorded from eight 40μm microwires inserted into a clinical electrode as described previously [1, 2]. Only data acquired from recording contacts within the amygdala are reported here. Electrodes were positioned such that their tip lands in the upper third to center of the deep amygdala, about 7 mm from the uncus [4, 5]. Efforts were always made to avoid passing the electrode through a sulcus, and its attendant sulcal blood vessels, and thus the location varied but was always well within the body of the amygdala. Microwires projected medially out at the end of the depth electrode and examination of the microwires after removal suggests a spread of about 20-30 degrees. The electrodes were thus likely sampling neurons in the mid-medial part of the amygdala and the most likely microwire location is thus the basomedial nucleus or possibly the deepest part of the basolateral nucleus. Bipolar wide-band recordings (0.1-9kHz), using one of the eight microwires as reference, were sampled at 32 kHz and stored continuously for off-line analysis with a 64-channel Neuralynx system (Digital Cheetah; Neuralynx, Inc.). The raw signal was filtered with zero-phase lag 300-3kHz bandpass filter and spikes were sorted using a semi-automatic template matching algorithm as described previously [6]. Channels with interictal epileptic spikes in the LFP were excluded. For wires which had several clusters of spikes (74 wires had at least one unit, 51 of which had at least two), we additionally quantified the goodness of separation by applying the projection test [6] for each possible pair of neurons. The projection test measures the number of standard deviations by which the two clusters are separated after normalizing the data, so that each cluster is normally distributed with a standard deviation of 1. The average distance between all possible pairs (n = 294) was 12.1±6.7 standard deviations. The average SNR of the mean waveforms relative to the background noise was 2.2±0.1 and the average percentage of inter-spike intervals that were less than 3ms (a measure of sorting quality) was 0.25±0.02%.

Stimuli and Task

Patients were asked to judge whether faces (or parts thereof) shown for 500ms are happy or fearful (2-alternative forced choice). Stimuli were presented in blocks of 120 trials (see Fig. 1).

Stimuli consisted of bubbled faces (60% of all trials), eye region (left and right, 10% each), mouth region (10% of all trials), or whole (full) faces (10% of all trials) and were shown randomly interleaved at the center of the screen of a laptop computer situated at the patient's bedside. Mouth and eye region stimuli were all the same size. Each trial consisted of a sequence of images shown in the following order: 1) scrambled face, 2) face stimulus, 3) blank screen. Scrambled faces were created from the original faces by randomly re-ordering their phase spectrum. They thus had the same amplitude spectrum and average luminance. Scrambled faces were shown for 0.8-1.2s (randomized). Immediately afterwards, the target stimulus was shown for 0.5s (fixed time), which was then replaced by a blank screen. Subjects were instructed to make their decision as soon as possible. Regardless of reaction time (RT), the next trial started after an interval of 2.3-2.7s after stimulus onset. If the subject did not respond by that time, a timeout was indicated by a beep (2.2% of trials were timeouts and were excluded from analysis). Patients responded by pressing marked buttons on a keyboard (happy or fearful). Distance to the screen was 50 cm, resulting in a screen size of 30° X 23° of visual angle and a stimulus size of approximately 9° squared of visual angle. The average luminance at the center of the screen was 19.6±1.3, 24.7±0.5, and 17.7±0.8 lux for bubbled, whole faces and scrambles, respectively (the maximal luminance of the screen with pixel values on maximally was 43 lux). Patients completed 5-7 blocks during which we collected electrophysiological data continuously. After each block, the achieved performance was displayed on a screen to participants as an incentive.

Bubbles stimuli were constructed as described previously [7]. We used 8 face base images (chosen from the Ekman and Friesen stimulus set, 4 different individuals (2 female and 2 male) showing happy and fearful expressions each, all normalized for mean luminance, contrast, and position of eyes and mouth; a random subset of 50% of stimuli were randomly flipped along the vertical axis to prevent any influence of left-right asymmetries present in the faces, resulting in 16 different face images. Note that for each individual, both a fearful and a happy face was part of the dataset, making it impossible for subjects to learn a strategy of identifying the faces instead of performing the emotional categorization task.

These face stimuli were then sparsely sampled and presented to participants in the bubbles trials (Fig. 1A). Each bubble was a symmetric 2D Gaussian with σ=10 pixels. The number of bubbles shown was adapted continuously using the QUEST-staircase method with β=3.5, δ=0.01 and γ=0.5 [8] targeting an error rate of 20% (the error trials were used to compute the classification image, see below). The mean asymptotic performance actually obtained was 82.6%, confirming the validity of the adaptive procedure. The location of each bubble was chosen randomly and independently of all other bubbles. As subjects improved, the number of bubbles required decreased (learning curve, Fig 1B). The same 8 faces were also used for the whole face and eye/mouth region trials. Patients performed a short training version of the task (data not included) before the experiment with the same stimuli to familiarize them with the task. We implemented the task with the Psychophysics Toolbox [9].

Eye Movements

We recruited an independent group of 30 healthy subjects at the California Institute of Technology (all undergraduate students) to check that eye movements to the bubbles stimuli were not grossly different from those to whole faces. Participants viewed the same stimuli as patients while their eye movements were recorded using a head-mounted EyeLinkII system (SR Research, Canada). The number of bubbles revealed was adjusted on a trial-by-trial basis as

described above, starting with 50 bubbles. Two fixation density maps were calculated for each subject: one for the full face and one for the bubbled condition. Density maps were calculated based on the number and location of all fixations during the 500ms long stimulus presentation and convolved with a Gaussian kernel with σ=10 pixels. We compared density maps between the full-face and bubbled conditions by computing the mean and variance of the density maps separately along the x-and y-axes for every subject.

Data Analysis: Behavior

Classification images (CI) were derived as described previously [7]. Briefly, the CIs were calculated for each session based on accuracy and RT. Only bubble trials were used. Each pixel C(x,y) of the CI is the correlation of the noise mask at that pixel with whether the trial was correct/incorrect or the RT (Eq 1). Pixels with high positive correlation indicate that revealing this pixel increases task performance. The raw CI C(x,y) is then rescaled (z-scored) such that it has a student's-t distribution with N-2 degrees of freedom (Eq 2).

$$C(x,y)=\sum_{i=1}^{N}\frac{[X_i(x,y)-\overline{X}(x,y)](Y_i-\overline{Y})}{\sqrt{\sum_{j=1}^{N}[X_j(x,y)-\overline{X}(x,y)]^2}\sqrt{\sum_{j=1}^{N}(Y_j-\overline{Y})^2}} \quad \text{(Eq 1)}$$

$$Z(x,y)=\sqrt{n}C(x,y) \quad \text{(Eq 2)}$$

N is the number of trials, $X_i(x,y)$ is the smoothened noise mask for trial i, Y_i the response or the reaction time for trial i and $\overline{X}(x,y)$ and $\overline{Y}$ is the mean over all trials. The noise masks $X_i(x,y)$ are the result of a convolution of bubble locations (where each center of a bubble is marked with a 1, and all other pixel values are set to 0) with a 2D Gaussian kernel with width σ=10 pixels and a kernel size of 6σ. Before convolution, images were zero-padded to avoid edge effects. For each session, we calculated two CIs: one based on accuracy and one based on RT. These were then averaged as $Z(x,y)=[Z_{RT}(x,y)+Z_{accuracy}(x,y)]/\sqrt{2}$ to obtain the CI for each session. CIs across session were averaged similarly, resulting in the behavioral CI shown in Fig 1C.

Data Analysis: Spikes

Only units with an average firing rate of at least 0.2 Hz (entire task) were considered. Only single units were considered (see Electrophysiology for classification details). For analysis, only correct trials were considered and all raster plots only show correct trials. However, we also re-ran all our analyses with the inclusion of both correct and incorrect trials and results were qualitatively similar (not shown). The first 10 trials of the first block were discarded from analyses. Trials were aligned to stimulus onset, except when comparing the baseline to the scramble-response for which trials were aligned to scramble onset (which precedes the stimulus onset). Statistical comparisons between the firing rates in response to different stimuli were made based on the total number of spikes produced by each unit in a 1s interval starting at 250ms after stimulus onset. Pairwise comparisons were made using a two-tailed t-test at $p<0.05$ and Bonferroni-corrected for multiple comparisons where necessary (as noted). Average firing rates (PSTH) were computed by counting spikes across all trials in consecutive 250ms bins. To convert the PSTH to an instantaneous firing rate, a Gaussian kernel with sigma 300ms was used (for plotting purposes only, all statistics are based on the raw counts).

Data Analysis: Face Responses for Whole Faces

We quantified for each recorded unit how much its response differed between whole faces and partially revealed faces using a whole-face index (WFI). The WFI of unit i is the baseline normalized difference in mean response to whole faces trials compared to bubbles trials (Eq 3).

$$WFI_i = \frac{\overline{R}_{WholeFace} - \overline{R}_{Bubbles}}{\overline{R}_{Baseline}} 100\% \qquad \text{(Eq 3)}$$

If the WFI is different from 0, the unit responds to whole-faces differently than to partially revealed faces. Note that a high WFI, regardless whether negative or positive, indicates whole-face-selective responses.

Data Analysis: Selection of Whole-Face Selective Units

Units were classified as whole-face selective if their firing rate differed significantly between whole-face trials and eye/mouth cutout trials. Further, WF-selective units were classified as either increasing or decreasing their rate based on the same trials (i.e. if the whole-face trials had a higher rate compared to cutout trials, the unit was classified as increasing). All subsequent statistics (such as the WFI, see above) were based on the bubbles trials and not the cutout trials, thus making these measures statistically independent.

Data Analysis: Face Responses for Partially Revealed Faces

For population averages and quantification of responses relative to whole-face responses, the spike rate of each unit was normalized to the average number of spikes obtained to whole faces in a 1s window starting 250ms after stimulus onset (making the response to a whole face trial equal to 1.0 on average). For the bubbles trials, we quantified, for each unit, the number of spikes as a function of the proportion of pixels revealed of the total face, as well as the proportion of pixels revealed within ROIs only around both eyes and the mouth of the stimulus (see Fig 4A). The reasons we chose these ROIs in addition to quantifying the amount of the entire face was: (1) the eyes and mouth ROI in fact contained the information on the basis of which subjects performed the face discrimination task in our experiment, as demonstrated by the classification images shown in Figure 1C; (2) we were interested in comparing responses to whole faces with responses to their key features, in particular eyes and mouth; (3) while %ROI and %whole face shown were correlated, there was a lot of scatter as well and there was a greater range of ROIs revealed in the bubbles than whole face revealed. If every pixel in the 3 ROIs was revealed, or every pixel of the entire face was revealed, our measure equals 100%.

We calculated the response of individual units or the population as a function of the proportion of the ROI revealed (%ROI revealed in Fig 4) in bins of 15% with a step-size of 5%. Only bins consisting of at least 10 trials were considered and are otherwise not shown. The first 150 trials were excluded for this calculation to eliminate novelty effects and the large change in bubbles that occurred in this epoch (cf. Fig 1B). Including all trials, however, results in qualitatively very similar results. This measure could not be calculated for all individual units, particularly for rare trials in which a large proportion of the face or ROIs were revealed, but could be obtained in all cases for the population average. For each unit, we tested for a significant association between the percentage of the face revealed and spike rate with a linear regression between the number of spikes evoked and the proportion of the face revealed. The

slope of the regression line was further considered only if the regression was statistically significant ($p<0.05$). We verified the robustness of the resulting slope using a bootstrap statistic [10] either over trials or units, each with 1000 replications. For each of the bootstrap samples, we calculated the regression slope of the resulting population (Histograms in Fig 4C,D). The sign of the slope was highly robust across both bootstrap samples. Slopes are specified in terms of normalized rate per 100% ROI (i.e. the change in rate when going from 0% ROI to 100% ROI). Note that since bubbles locations are chosen independently of one another, the proportion of any individual ROI revealed is positively correlated with the proportion of all other ROIs revealed (since more of the entire face is shown whenever there are more bubbles on a given trial, illustrated in Fig S3).

Finally, we also modeled for each bubble trial and whole-face trial the spatial contrast (the perceptual threshold for detecting foveal spatial contrast variation) using a model described previously (Watson and Ahumada 2005). This gives us one measure of a low-level visual property of the stimuli, their (modeled) perceptual spatial detection threshold required for this stimulus to be detectable. The higher the threshold, the more difficult it is to recognize the stimulus.

All data analysis was performed using custom written routines in MATLAB. All errors are ±s.e.m., unless specified otherwise.

Supplemental References

1. Rutishauser, U., Ross, I.B., Mamelak, A.N., and Schuman, E.M. (2010). Human memory strength is predicted by theta-frequency phase-locking of single neurons. Nature *464*, 903-U116.
2. Rutishauser, U., Mamelak, A.N., and Schuman, E.M. (2006). Single-trial learning of novel stimuli by individual neurons of the human hippocampus-amygdala complex. Neuron *49*, 805-813.
3. Benton, A.L., Hamsher, K., Varney, N.R., and Spreen, O. (1983). Contributions to Neuropsychological Assessment, (New York: Oxford University Press).
4. Amunts, K., Kedo, O., Kindler, M., Pieperhoff, P., Mohlberg, H., Shah, N.J., Habel, U., Schneider, F., and Zilles, K. (2005). Cytoarchitectonic mapping of the human amygdala, hippocampal region and entorhinal cortex: intersubject variability and probability maps. Anat Embryol (Berl) *210*, 343-352.
5. Oya, H., Kawasaki, H., Dahdaleh, N.S., Wemmie, J.A., and Howard, M.A., 3rd (2009). Stereotactic atlas-based depth electrode localization in the human amygdala. Stereotact Funct Neurosurg *87*, 219-228.
6. Rutishauser, U., Schuman, E.M., and Mamelak, A.N. (2006). Online detection and sorting of extracellularly recorded action potentials in human medial temporal lobe recordings, in vivo. Journal of neuroscience methods *154*, 204-224.
7. Gosselin, F., and Schyns, P.G. (2001). Bubbles: a technique to reveal the use of information in recognition tasks. Vision Research *41*, 2261-2271.
8. Watson, A.B., and Pelli, D.G. (1983). Quest - a Bayesian Adaptive Psychometric Method. Percept Psychophys *33*, 113-120.
9. Brainard, D.H. (1997). The Psychophysics Toolbox. Spatial Vision *10*, 433-436.
10. Efron, B., and Tibshirani, R.J. (1993). An Introduction to the Bootstrap, (London: Chapman&Hall).